Observation of full shot noise in CoFeB/MgO/CoFeB-based magnetic tunneling junctions

K. Sekiguchi,[1,a)] T. Arakawa,[1] Y. Yamauchi,[1] K. Chida,[1] M. Yamada,[2] H. Takahashi,[2] D. Chiba,[1] K. Kobayashi,[1] and T. Ono[1]
[1]*Institute for Chemical Research, Kyoto University, Uji 611-0011, Japan*
[2]*Advanced Research Laboratory, Hitachi Ltd., Kokubunji, 185-8601 Tokyo, Japan*

(Received 16 May 2010; accepted 2 June 2010; published online 23 June 2010)

The electron transport through the CoFeB/MgO/CoFeB-based magnetic tunneling junction (MTJ) was studied by the shot noise measurement. The obtained Fano factor to characterize the shot noise is very close to unity, indicating the full shot noise, namely, the shot noise in the Schottky limit, both in the parallel and antiparallel magnetization configurations. This means the Poissonian process of the electron tunneling and the absence of the electron–electron correlation in the low bias regime. The shot noise measurements will be a good guideline to make up tunneling criteria for designing MTJ-based spin devices. © *2010 American Institute of Physics*. [doi:10.1063/1.3456548]

The tunneling magnetoresistance (TMR) is one of central topics in spintronics, which is invoking intensive studies on the realizations of sensitive magnetic sensors and microwave oscillators.[1] In terms of the electron tunneling in magnetic tunneling junctions (MTJs), the spin-dependent electron tunneling based on the simple Julliere's model[2] is applicable in the transport through amorphous Al_2O_3 junctions,[3] whereas the coherent tunneling is expected in epitaxial MgO (100) junctions.[4–7] The large spin polarization plays a critical role in CoFeB/MgO/CoFeB junctions.[8,9] In addition to the conventional resistance measurement, the shot noise measurement allows us to explore more the underlying physics of electron transport.[10] For example, the shot noise has served to prove the fractional charge in the fractional quantum Hall regime[11,12] and the Cooper-pair transport in the superconductor-normal junctions.[13] Similarly, a spin-related electron dynamics such as spin transfer torque is expected to emerge itself in the shot noise.[14–17]

Generally, when the current I is fed to a junction with the resistance, the current noise S_I across it due to the shot noise can be expressed as $S_I=2eIF$ (in the zero-temperature limit) with the Fano factor F. $F=1$ in conventional Schottky-type junctions. Although there are several papers on the $1/f$ noise in MTJs,[18–22] so far only a few studies are available on the Fano factor. One of them reported a distinct suppression of Fano factor ($F\sim0.45$) in Al_2O_3-based MTJs (Ref. 22) after reporting $F\sim1$.[23] Another group reported that the shot noise in Al_2O_3-based MTJs with Cr doped barrier shows $F\sim0.65$.[24] Thus, the Fano factor for the MTJs remains unsettled and also that for MgO-based MTJs is not known yet.

Here we report the systematic study on the shot noise in MgO-based MTJs. The observed Fano factor indicates the full shot noise in the MTJs, signaling that the spin-dependent Poissonian process governs the electron transport. We also revealed that the magnetization fluctuation is the main origin of $1/f$ noise in MTJs.

Our MTJs consist of Ta(3) / Cu(50) / IrMn(10) / CoFeB(2.5) / Ru(0.8) / CoFeB(3) / MgO(1.5) / CoFeB(4) / Ta(2) / Ru(5) / Cu(3) / Au(100) multilayer stacks grown by magnetron sputtering on SiO_2 layer on a silicon substrate [see Fig. 1(a)]. Here the numbers in () indicates the thickness of each layer in units of nanometer. The multilayer stacks are patterned into 2×2 and 5×5 μm^2 junctions by the electron beam lithography, then annealed in 0.6 T for 60 min at 350 °C to improve the crystallization of the amorphous ferromagnetic CoFeB layers,[8,9] yielding high TMR ratios exceeding 150%. The area resistance (RA) ranges from 500 $\Omega/\mu m^2$ to 50 $k\Omega/\mu m^2$.

The shot noise measurements were carried out in a variable temperature insert (Oxford VTI) as schematically shown in Fig. 1(a). The dc current is applied to the MTJ through a 10 MΩ resistor. The two voltage signals across the MTJ in the cryostat are obtained through a pair of the voltage probes in an electronic circuits optimized for the present MTJ resistance (typically a few kilohm). Each signal is consecutively amplified by the room temperature amplifiers (NF corpora-

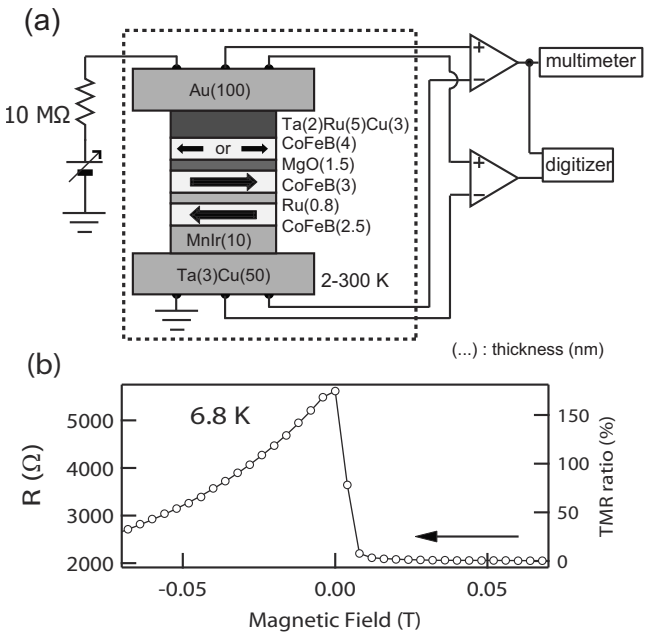

FIG. 1. (a) The present MTJs consist of Ta(3) / Cu(50) / IrMn(10) / CoFeB(2.5) / Ru(0.8) / CoFeB(3) / MgO(1.5) / CoFeB(4) / Ta(2) / Ru(5) / Cu(3) / Au(100) multilayer. The resistance and the noise measurement setups are schematically shown. (b) Typical resistance of the MTJ measured at 6.8 K. The arrow shows the direction of the field sweep.

[a)]Electronic mail: koji_s@scl.kyoto-u.ac.jp.

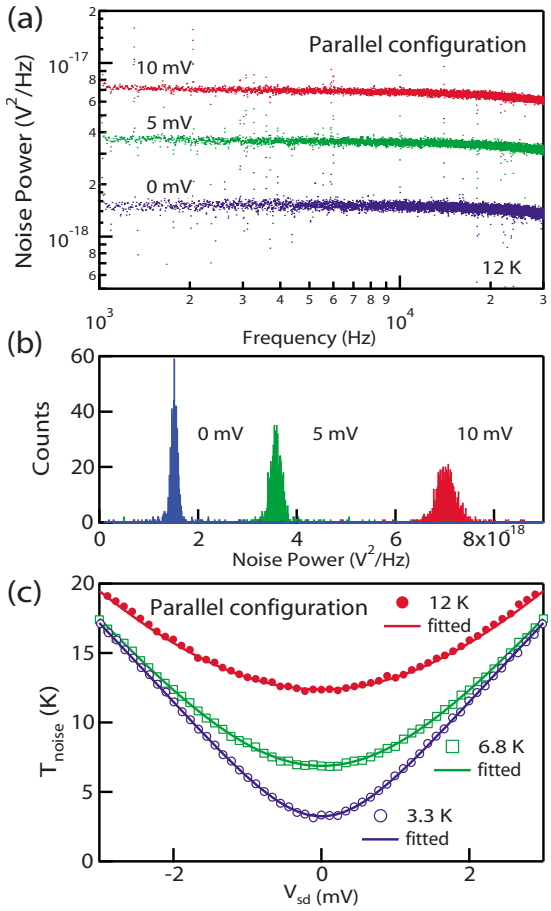

FIG. 2. (Color online) (a) Noise spectral density $S_V(f)$ for the P magnetization configuration at $V_{sd}=0$, 5, and 10 mV. (b) Histograms of the noise power spectral density between 1 and 5 kHz. (c) Noise power as a function of bias voltage expressed in terms of the noise temperature T_{noise}.

tion LI-75A with the input referred noise is 2 $\text{nV}/\sqrt{\text{Hz}}$), and recorded at the two-channel digitizer (National Instruments PCI-5922). In order to increase the resolution, the measured two sets of the time domain data are cross-correlated with yield the noise power spectral density through the fast Fourier transformation technique. The temperature of the samples is derived from the thermal noise measurement. We have measured the shot noise from four different MTJs between 3 and 20 K, which gives essentially the same result regarding the Fano factor and the $1/f$ noise as discussed below.

Figure 1(b) shows the typical characterization of our MTJs at low temperatures. The resistance of MTJ at the lowest resistance state (parallel magnetization configuration; P) is 2.05 kΩ, while the highest resistance state (antiparallel magnetization configuration; AP) is 5.61 kΩ [Fig. 1(b)]. The TMR ratio defined by $(R_{\text{AP}}-R_{\text{P}})/R_{\text{P}}$ is 173%. The shot noise measurement is performed with changing a magnetic field (typically measured at P and AP states). Although the differential resistance in the AP configuration shows a peak feature around zero bias voltage,[23,24] for the noise measurement we focus ourselves on the sufficiently low bias regime below a few millivolt, where the differential resistance is treated as constant. By using a numerical fitting of the $I-V$ curves,[25] the barrier height of the present MgO is evaluated to be 0.22 eV, being consistent with the previous results.

Figure 2 shows the typical voltage noise power spectra $S_V(f)$ as a function of the frequency for the P configurations for the bias voltages $(V_{sd})=0$, 5, and 10 mV at 12 K. Except several spikes observed at certain frequencies, which are due to external noises, the spectra are flat between 1 and 5 kHz. At high frequencies ($\gg 10$) kHz the RC damping of the voltage noise due to the finite capacitance (~700 pF) of the measurement lines occurs. The frequency independent contribution observed in the spectrum at $V_{sd}=0$ mV is attributed to the Johnson–Nyquist (thermal) noise. To estimate the amplitude of this frequency-independent noise, we performed the histogram analysis of the number of the points between 1 and 5 kHz as shown in Fig. 2(b). The center of the Gaussian fit of the obtained histograms gives a better estimation for the average noise power than just the average of the spectrum, since unwanted peaks, which accidentally appear in the spectra, do not very much contribute in the histogram. Thus from the histogram obtained for $V_{sd}=0$ mV the electron temperature of the MTJ can be deduced by using the device resistance, as the thermal noise is given as $S_V=4k_BTR$ where k_B, T, and R are Boltzmann constant, sample temperature, and resistance, respectively.

By increasing the bias voltage at a fixed temperature, the shot noise, which is also frequency-independent at a low frequency range as in the present study, appears as the increase of the noise power. Again, the shot noise on top of the thermal noise can be precisely evaluated by the histogram analysis. As an example, Fig. 2(b) shows the histograms obtained for $V_{sd}=5$ and 10 mV, where the difference of the center position of the histogram from that at $V_{sd}=0$ mV corresponds to the shot noise.

Figure 2(c) represents the noise power S_V for the same MTJ for three different temperatures (3.3, 6.8, and 12 K as estimated from the thermal noise). Here we express S_V by using the noise temperature $T_{\text{noise}}\equiv S_V/4k_BR$ to absorb the slight resistance difference for different temperatures. While the thermal noise contribution is dominant around $V_{sd}=0$ mV, the parabolic behavior at finite bias indicates the crossover from the thermal to the shot noise. At large enough bias voltages ($eV_{sd}\gg k_BT$), the noise power increases linearly to the bias voltage as $S_V=2eFRV_{sd}$, where F is the Fano factor. To obtain the Fano factor, we performed the numerical fitting to take the crossover between the thermal noise and the shot noise into account by using the following equations,[10]

$$S_V = 4k_BTR + 2FR\left[eV_{sd}\coth\left(\frac{eV_{sd}}{2k_BT}\right) - 2k_BT\right]. \quad (1)$$

From the numerical fitting line, we deduced $F=0.98$ for the three temperatures. The accuracy of the fitting also ensures that the effect of Joule heating in the MTJ is negligible.

The noise power spectra for the AP configuration for the same device are shown in Fig. 3(a). In contrast to the spectra obtained for the P configuration, they show a considerable $1/f$ contribution when the MTJ is voltage-biased. To obtain the frequency-independent contribution, we numerically fit the spectra by the function $(a+b/f)/[1+(f/f_c)^2]$, which includes the frequency-independent contribution a representing the thermal noise and the shot noise, and the $1/f$ contribution (b/f) with the RC-damping with the cut-off frequency f_c. The result of the fitting are superposed on the experimental curves by the solid curves in Fig. 3(a). After subtracting the $1/f$ contribution, we again performed the histogram analysis at low frequencies well below f_c to obtain the thermal and

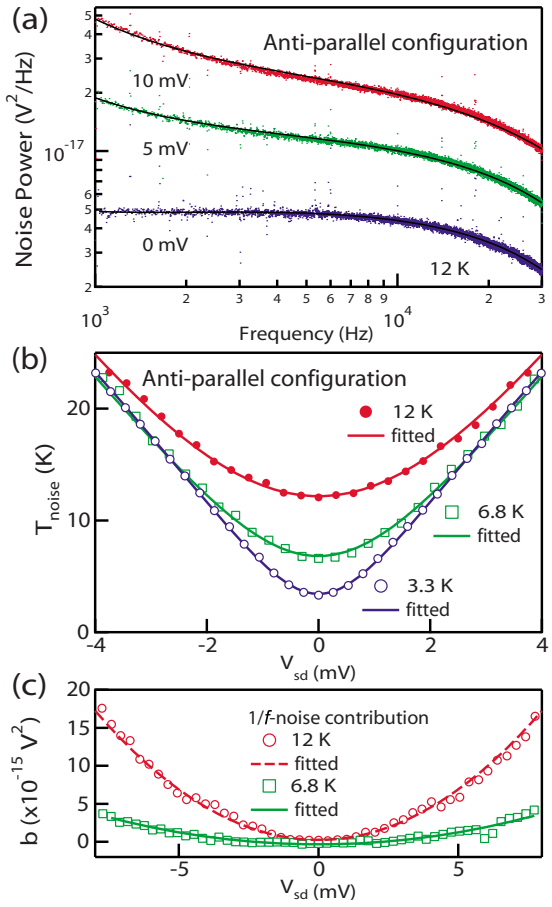

FIG. 3. (Color online) (a) Noise spectral density $S_V(f)$ for the AP magnetization configuration at V_{sd}=0, 5, and 10 mV. (b) Noise power as a function of bias voltage expressed in terms of the noise temperature T_{noise}. (c) $1/f$ contribution as a function of V_{sd}.

the shot noise. The obtained noise power as a function of the bias voltages are shown in Fig. 3(b) for three temperatures. The numerical fitting gives the Fano factor to be 1.00, 0.98, and 1.05 for 3.3 K, 6.8 K, and 12 K, respectively. Again, these values are very close to unity as well as in the P configuration.

Although the Fano factor in the MTJs has been discussed before, there seems some controversy. Jiang *et al.*[23] reported an observation of the full shot noise (i.e., $F \sim 1$) in MTJ's with AP alignment of electrodes. Later, the same group reported a strong suppression of F to be 0.45 in MTJs.[22] The first systematic study on the shot noise in MTJ was reported by Guerrero *et al.*[24] They observed significant suppression of the Fano factor ($F \sim 0.65$) in the amorphous Al_2O_3-based junctions, and discussed a possible role of the localized states that are uncontrollably formed within the barrier, because such localized states may act as nonmagnetic and/or paramagnetic impurity levels, leading to the suppression of the Fano factor. On the other hand, the present MgO-based junction consists of a well-crystallized interface presumably free from such localized states due to recrystallization by the annealing, as manifested in the high TMR ratio. Thus, our observation is believed intrinsic to the electron tunneling across TMR.

Finally, we discuss the $1/f$ noise in our device. From the numerical fitting of the obtained spectra, we deduce the $1/f$ noise (b/f) as a function of the bias voltage as shown in Fig. 3(c). Although b is zero at 3.3 K regardless of V_{sd} within the experimental accuracy, b becomes larger as V_{sd} and the temperature increase. As usually expected for the $1/f$ noise, b shows a parabolic behavior as a function of V_{sd} and the Hooge parameter $h=AfS_{1/f}/V_{sd}^2$ is deduced, where A is the junction area, and $S_{1/f}(f)$ is the $1/f$ noise power density. For the data shown in Fig. 3(c), h is 1.2×10^{-9} μm^2 and 6.2×10^{-9} μm^2 for 6.8 K and 12 K, respectively. These values are comparable to the previous report, where the origin of $1/f$ is speculated to be the local charge trap in the vicinity of a tunneling barrier. This is, however, not the case in the present experiment, since the $1/f$ noise is absent in the P configuration as shown in Fig. 2(a), which suggests that the $1/f$ noise in MTJs is revealed to be of magnetic origin. The possible mechanism is a magnetostriction of ferromagnetic layers as discussed before,[19] where the magnetoelastic constriction and/or elongation of the soft ferromagnetic layer may play a role following the field inversion.

In conclusion, the full shot noise is observed in the CoFeB/MgO/CoFeB-based MTJs, indicating that the tunneling mechanism can be described as an ideal Schottky type. By evaluating the Hooge parameter, the contribution of $1/f$ noise is identified to be of magnetic origin.

This work was supported by JSPS/MEXT.

[1]S. Yuasa, J. Phys. Soc. Jpn. **77**, 031001 (2008).
[2]M. Julliere, Phys. Lett. A **54**, 225 (1975).
[3]T. Miyazaki and N. Tezuka, J. Magn. Magn. Mater. **139**, L231 (1995).
[4]S. Yuasa, T. Nagahama, and Y. Suzuki, Science **297**, 234 (2002).
[5]S. Yuasa, T. Nagahama, A. Fukushima, Y. Suzuki, and K. Ando, Nature Mater. **3**, 868 (2004).
[6]S. S. Parkin, C. Kaiser, A. Panchula, P. M. Rice, B. Hughes, M. Samant, and S. H. Yang, Nature Mater. **3**, 862 (2004).
[7]W. H. Butler, X. G. Zhang, T. C. Schulthess, and J. M. MacLaren, Phys. Rev. B **63**, 054416 (2001).
[8]D. D. Djayaprawira, K. Tsunekawa, M. Nagai, H. Maehara, S. Yuasa, Y. Suzuki, and K. Ando, Appl. Phys. Lett. **86**, 092502 (2005).
[9]S. Yuasa, Y. Suzuki, T. Katayama, and K. Ando, Appl. Phys. Lett. **87**, 242503 (2005).
[10]Ya. M. Blanter and M. Buttiker, Phys. Rep. **336**, 1 (2000).
[11]R. de-Picciotto, M. Reznikov, M. Heiblum, V. Umansky, G. Bunin, and D. Mahalu, Nature (London) **389**, 162 (1997).
[12]L. Saminadayar, D. C. Glattli, Y. Jin, and B. Etienne, Phys. Rev. Lett. **79**, 2526 (1997).
[13]X. Jehl, M. Sanquer, R. Calemczuk, and D. Mailly, Nature (London) **405**, 50 (2000).
[14]A. L. Chudnovskiy, J. Swiebodzinski, and A. Kamenev, Phys. Rev. Lett. **101**, 066601 (2008).
[15]J. Foros, A. Brataas, G. E. W. Bauer, and Y. Tserkovnyak, Phys. Rev. B **75**, 092405 (2007).
[16]J. Foros, A. Brataas, G. E. W. Bauer, and Y. Tserkovnyak, Phys. Rev. B **79**, 214407 (2009).
[17]W. Wetzels, G. E. W. Bauer, and O. N. Jouravlev, Phys. Rev. Lett. **96**, 127203 (2006).
[18]J. Scola, H. Polovy, C. Fermon, M. Pannetier-Lecoeur, G. Feng, K. Fahy, and J. M. D. Coey, Appl. Phys. Lett. **90**, 252501 (2007).
[19]R. Guerrero, F. G. Aliev, R. Villar, J. Hauch, M. Fraune, G. Gunterodt, K. Rott, H. Bruckl, and G. Reiss, Appl. Phys. Lett. **87**, 042501 (2005).
[20]K. B. Klaassen, J. C. van Peppen, and X. Xing, J. Appl. Phys. **93**, 8573 (2003).
[21]S. Ingvarsson, G. Xiao, S. S. Parkin, W. J. Gallagher, G. Grinstein, and R. H. Koch, Phys. Rev. Lett. **85**, 3289 (2000).
[22]L. Jiang, J. F. Skovholt, E. R. Nowak, and J. M. Slaughter, Proc. SPIE **5469**, 13 (2004).
[23]L. Jiang, E. R. Nowak, P. E. Scott, J. Johnson, J. M. Slaughter, J. J. Sun, and R. W. Dave, Phys. Rev. B **69**, 054407 (2004).
[24]R. Guerrero, F. G. Aliev, Y. Tserkovnyak, T. S. Santos, and J. S. Moodera, Phys. Rev. Lett. **97**, 266602 (2006).
[25]J. G. Simmons, J. Appl. Phys. **34**, 238 (1963).